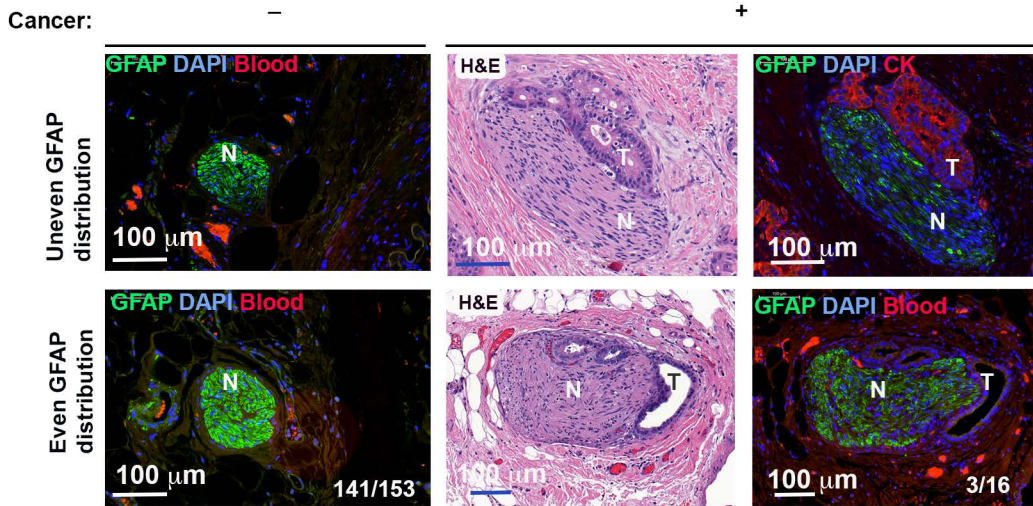
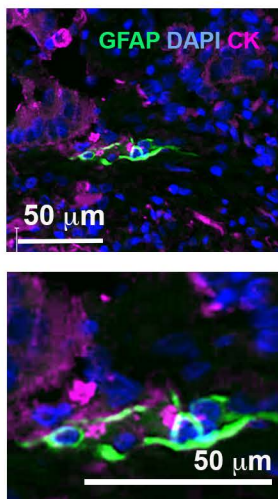


Supplementary Fig. 1 | Correlation of SC signatures and overall survival in patients with PAAD. A, Kaplan–Meier curves of overall survival (OS) and progression free survival (PFS) with high or low scores for different signatures of SC in 178 TCGA PAAD patients. **B,** Heatmap showing clustering of TCGA patients into 4 subtypes. **C,** SC signatures scores in the subtypes of the TCGA patients (S: squamous, P: progenitor, I: immunogenic, A: ADEX). **D,** Kaplan–Meier curves of overall survival (OS) with high or low scores for non-myelinating and myelinating SC signatures in short and long survivors MSK patients. **E, F,** Heatmaps of cell signatures correlating with scores for myelinating SC signature (E) and non-myelinating SC signature (F) in TCGA PAAD patients. **G,** Coefficient correlations between SC signature gene set and other gene sets in MSK and TCGA patients correlate with each other. **H,** Heatmaps of cell signatures correlating with scores for HEImix signature in TCGA PAAD patients.

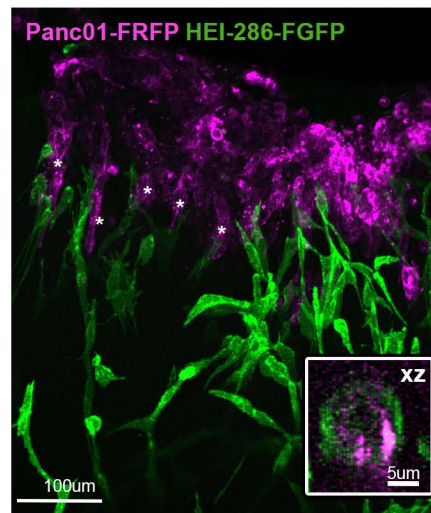
A



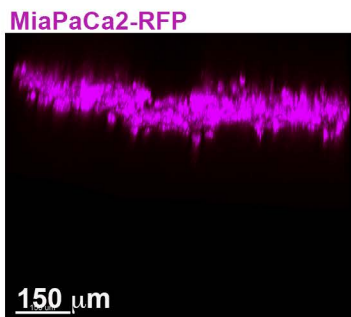
B



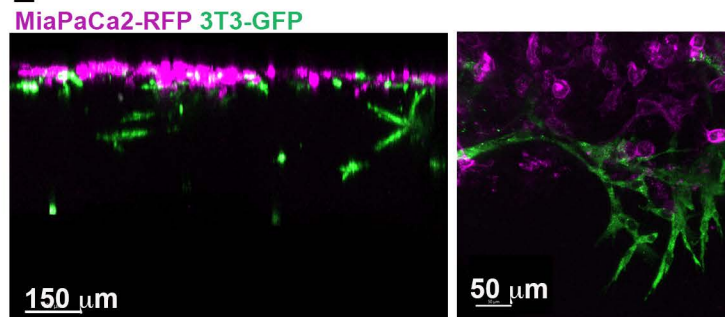
C



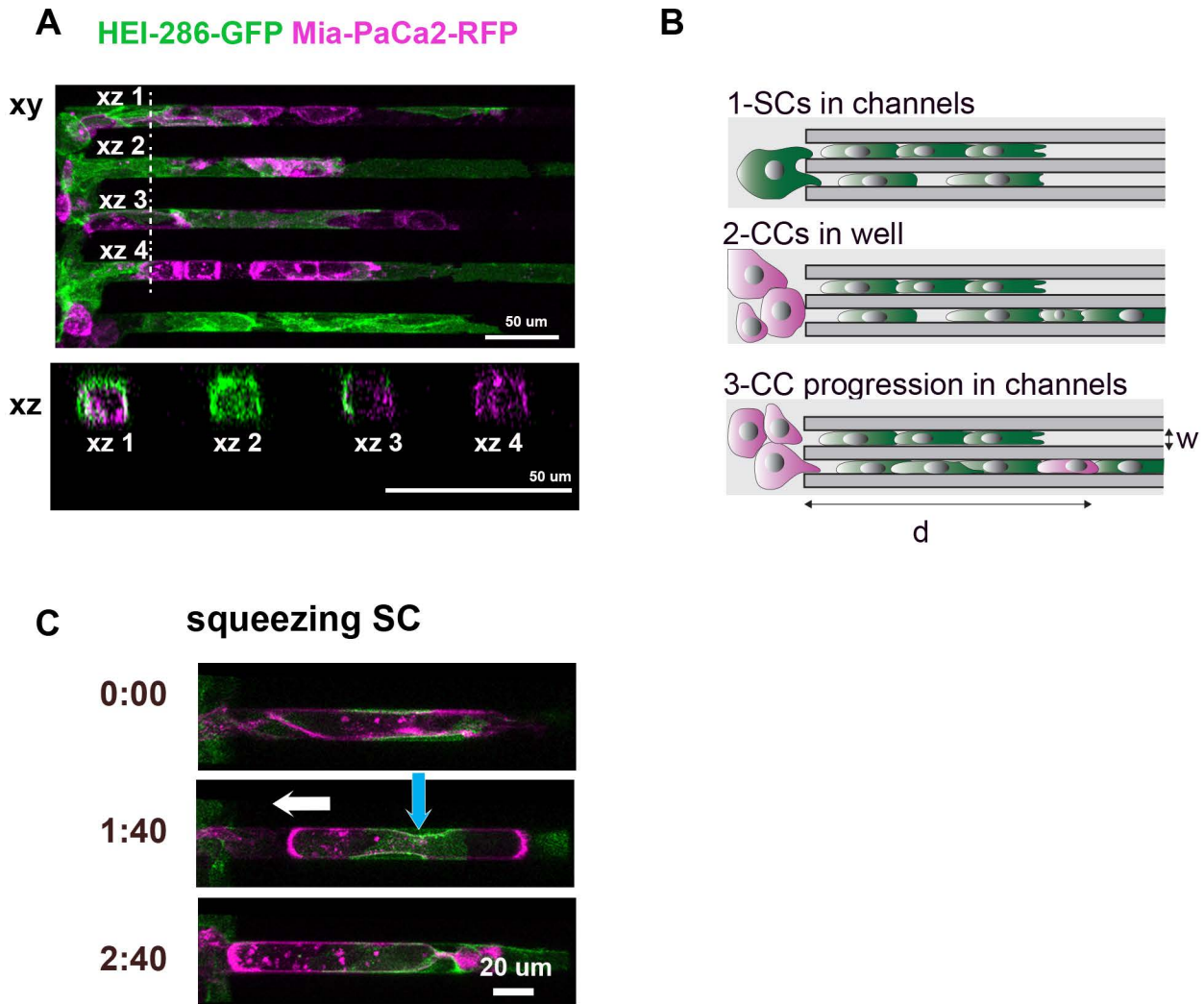
D



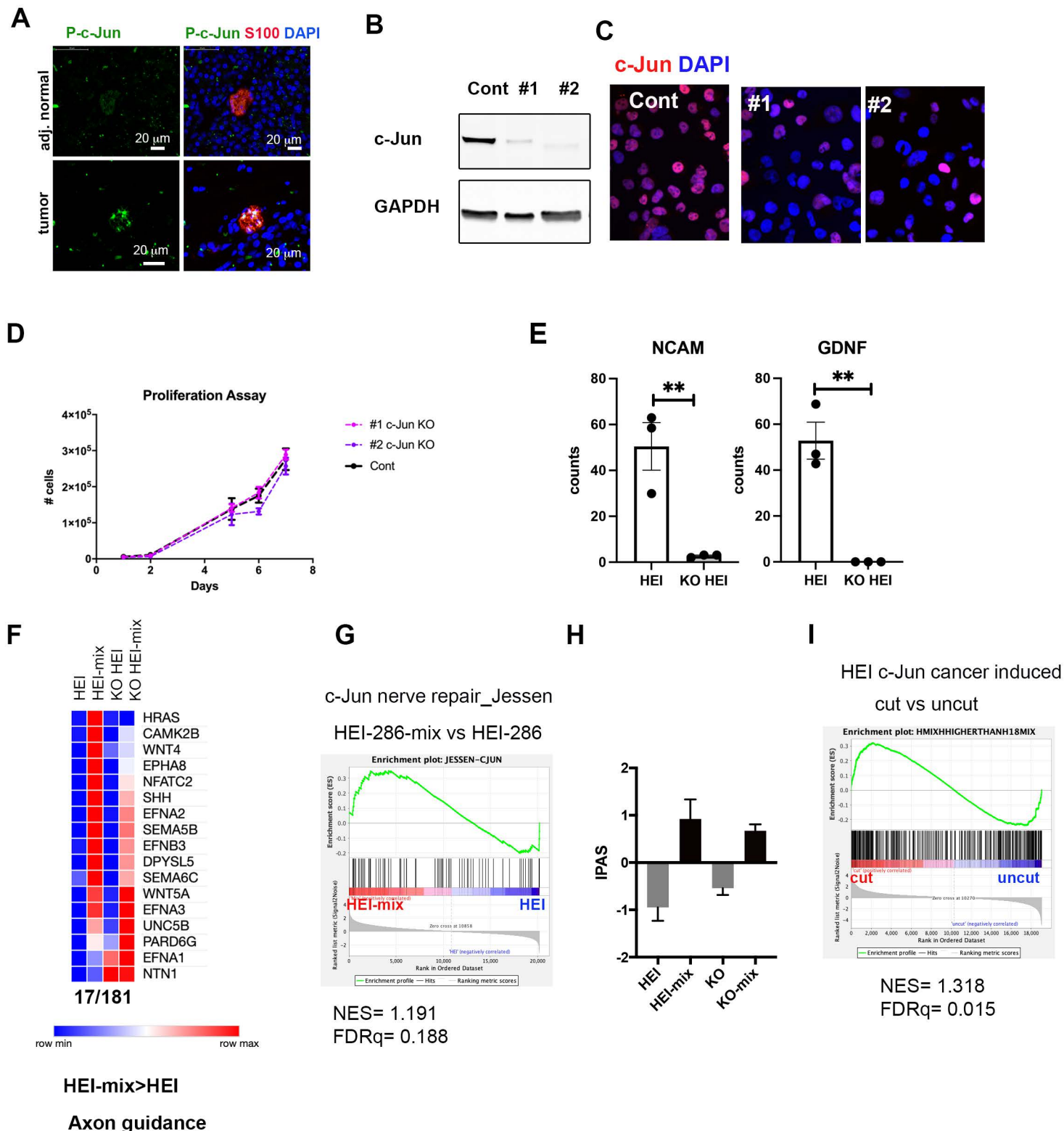
E



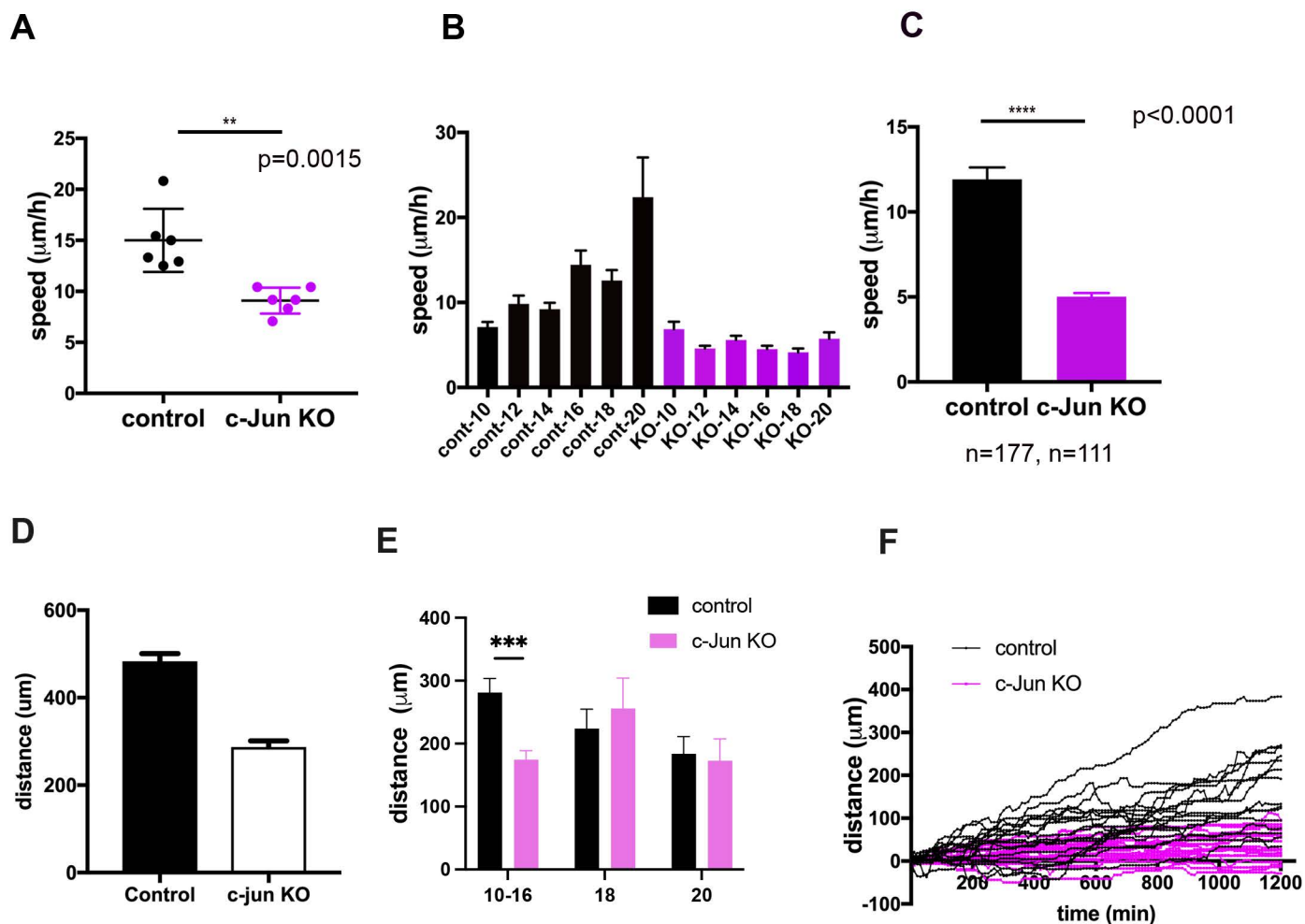
Supplementary Fig. 2 |Cancer cells are closely associated with SCs in PDAC specimens and do not invade in absence of SCs in a 3D assay. **A**, Examples of uneven (top) and even (bottom) distribution of GFAP (green) staining in nerves of PDAC specimens. Nerves without (left) and with (right) visible cancer cells. Middle images are H&E of adjacent sections of right images. Ratios (bottom right corner) indicate number of specimens with even GFAP distribution over the total number of specimens **B**, GFAP+ SC (green) wrapping cytokeratin (CK) expressing cancer cells (magenta) in PDAC specimen **C**, Confocal images showing Panc01 cancer cells (magenta) lined up with HEI-286 SCs (green) in Matrigel (see*). Inset: transverse image showing HEI-286 SCs wrapping around a Panc01 cancer cell. **D-E** Absence of chain of cancer cells in absence of SCs or with NIH 3T3 fibroblasts. **D**, Confocal images of MiaPaCa2-RFP cells seeded on top of a Matrigel chamber and imaged after 6 days. **E**, Confocal images of MiaPaCa2-RFP cells taken 6 days after adding them on top of a Matrigel chamber previously seeded with NIH 3T3-GFP fibroblasts for 5 days.



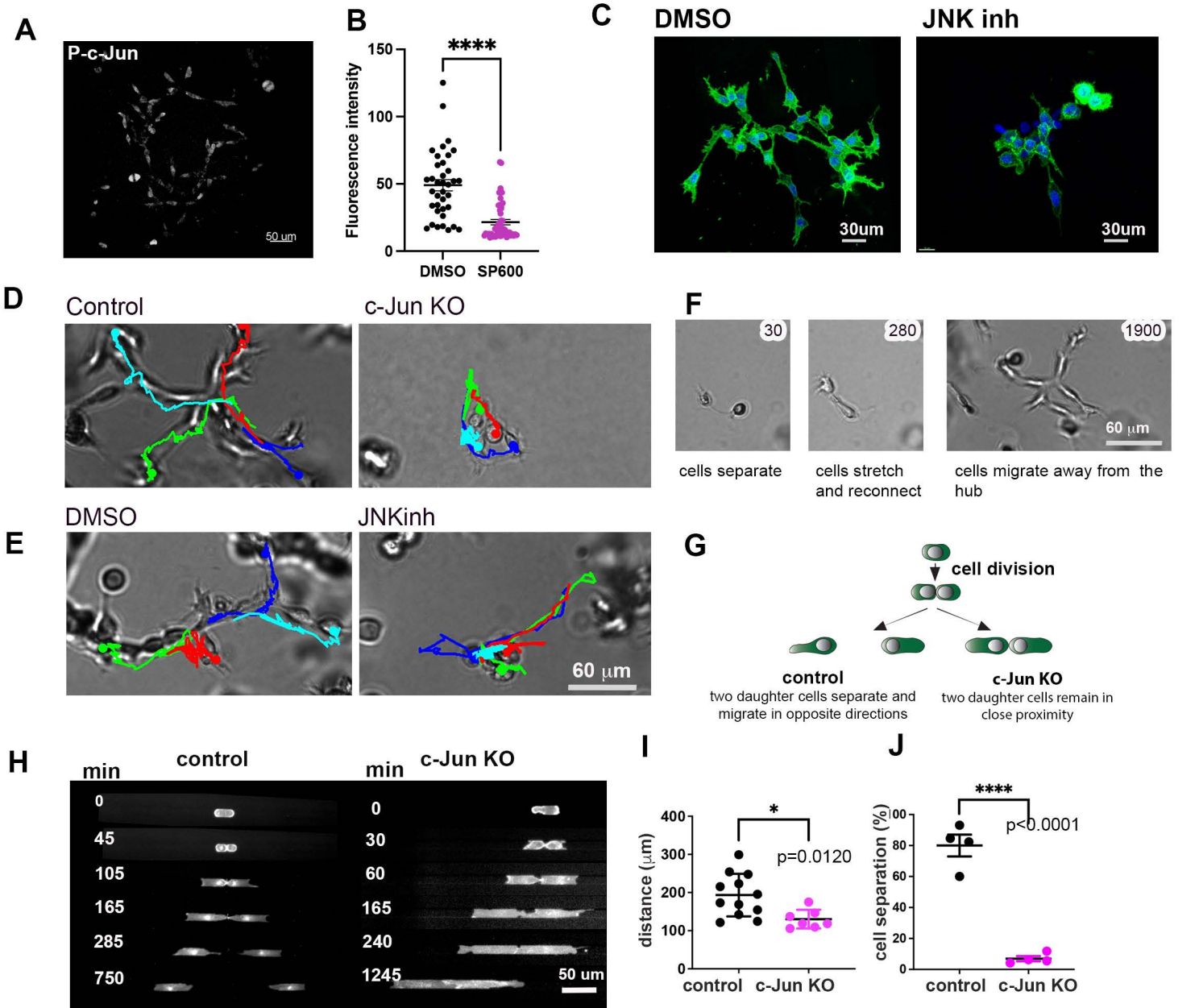
Supplementary Fig. 3 | HEI-286-GFP SCs and MiaPaCa-2-RFP cancer cell microchannel assay. A, Confocal images of HEI-GFP and MiaPaCa2-RFP within microchannels in longitudinal (xy) and transverse sections (xz) showing SCs fully occupying the channel (xz 2) or either wrapping partially (xz 3) or completely (xz 1) a cancer cell. **B,** Schematic showing the microchannel assay sequence. (1) HEI-286 SCs are first seeded in wells and enter microchannels. (2) MiaPaCa-2 cancer cells are seeded in the wells and (3) enter the microchannels occupied with HEI-286 SCs. **C,** Fluorescent images of time-lapse movie showing HEI-286 SCs (green) squeezing a cancer cell (magenta). Blue arrow indicates HEI-286 SC movement and white arrow indicates cancer cell displacement. Time is h:min.



Supplementary Fig. 4 | c-Jun and P-c-Jun in SCs. **A**, P-c-Jun staining in S100-labeled nerves from PDAC specimens that are close to tumor as compared with nerves from adjacent normal tissue. **B**, Western-Blot of HEI-286 SCs showing loss of c-Jun expression using either construct. **C**, Immunofluorescence of c-Jun in HEI-286 SCs showed diminished nuclear c-Jun expression with either construct. **D**, Proliferation of control and c-Jun KO HEI-286-SCs. **E**, mRNA expression level of NCAM1 and GDNF in HEI-286 and c-Jun KO HEI-286. **F**, Heatmaps of expression of axon guidance genes that are upregulated in co-cultured HEI-286 cells (HEI mix) as compared to HEI-286 grown alone (HEI). Each value is the mean of three biological replicates. **G**, Gene set enrichment analysis (GSEA) assessing upregulated c-Jun nerve-repair genes (27) in co-cultured HEI-286 compared to HEI-286 SCs. NES is normalized enrichment score. **H**, Inferred Pathway Activation/Suppression (IPAS) scores for the murine c-Jun nerve repair genes signature (27). **I**, GSEA assessing upregulated c-Jun genes in co-culture HEI versus grown alone HEI-286 in cut sciatic nerves compared to uncut sciatic nerves (27). NES is normalized enrichment score.



Supplementary Fig. 5 | SC c-Jun supports both SC and cancer cell migration. **A**, Quantification of control and c-Jun KO HEI-286-SC speed in two dimensions. **B**, Quantification of control and c-Jun KO HEI-286-SC speed in three dimensions in microchannels of sizes from 10 to 20 μm . **C**, Quantification of control and c-Jun KO HEI-286-SC speed in three-dimension. **D**, Quantification of length of columns formed by MiaPaCa-2 combined with WT HEI-286 SCs or with c-Jun KO HEI-286-SCs. **E**, Quantification of distance migrated by Panc01 cancer cells in microchannels of different widths, and occupied by HEI-286 SCs (n=18-35 cells per channel size). **F**, Individual tracks of cancer cells in microchannels occupied by control vs. c-Jun KO HEI-286 SCs. (n=21 in each group).



Supplementary Fig. 6 | WT and c-Jun KO SCs behavior. **A**, Confocal images of phospho-c-Jun (P-c-Jun) staining in HEI-286 GFP SCs in Matrigel. **B**, Effect of SP600125 on P-c-Jun expression in HEI-286 GFP SCs. **C**, Confocal images of HEI-GFP-SCs treated with JNKi SP600125 or DMSO in Matrigel showing lack of SC organization in JNKi-treated cells. **D-E**, Images of cells from 72h time-lapse movies of control and c-Jun KO HEI-286 SCs (**D**) and DMSO or JNK inhibitor treated HEI-286 SCs (**E**) grown in 3D Matrigel with colored cell tracking. **F**, Images of WT SCs from time-lapse movies showing formation of a branched organized structure in 3D: cells separate after division (1); cells stretch and reconnect, reestablishing contacts (2); cells divide, organize in a structure that spreads out (3). Time in minutes **G**, Schematic show the separation and positioning of two daughter HEI-286 SCs after mitosis in Matrigel is c-Jun-dependent. **H**, Time-lapse images of a dividing control and c-Jun-KO HEI-286 SCs and the two daughter cells in microchannels. **I**, Quantification of (**H**), the distance between two daughter cells following mitosis for control vs. c-Jun KO HEI-286 SCs in a 400 min time period (control $n=16$, c-Jun KO $n=12$, mean \pm SEM). **J**, Quantification of percentage of daughter cells that separate following mitosis for control versus c-Jun KO HEI-286 SCs. (4 independent experiments, $n>20$ cells per condition in each experiment, mean \pm SEM)